[CANCER RESEARCH 64, 3256–3264, May 1, 2004]

Ubiquitination and Proteasomal Degradation of Nucleophosmin-Anaplastic Lymphoma Kinase Induced by 17-Allylamino-Demethoxygeldanamycin: Role of the Co-Chaperone Carboxyl Heat Shock Protein 70-Interacting Protein

Paolo Bonvini, Henry Dalla Rosa, Nadia Vignes, and Angelo Rosolen

Clinica di Oncoematologia Pediatrica, Azienda Ospedaliera-Università di Padova, Padova, Italy

ABSTRACT

Nucleophosmin-anaplastic lymphoma kinase (NPM-ALK) is a constitutively active fusion tyrosine kinase involved in lymphomagenesis of human anaplastic large cell lymphomas (ALCL), the maturation and activity of which depend on the association with the heat shock protein (hsp) 90 protein chaperone. Targeting hsp90 by the ansamycins geldanamycin and 17-allyl-amino-demethoxygeldanamycin (17-AAG) promotes degradation of several proteins through the ubiquitin-proteasome pathway, including oncogenic Raf, v-Src, erbB2, and BCR-ABL. We have previously shown that 17-AAG prevents hsp90/NPM-ALK complex formation and fosters NPM-ALK turnover, perhaps through its association with the hsp70 chaperone. Here, we show that inhibition of the proteasome activity by the potent and specific compound pyrazylcarbonyl-Phe-Leu-boronate (PS-341) blocks 17-AAG-induced down-regulation of NPM-ALK, which becomes detergent-insoluble and relocates into ubiquitin-rich perinuclear vesicles that represent aggregated polyubiquitinated forms of the protein. Kinase activity was not mandatory for proteasomal degradation of NPM-ALK, because kinase-defective NPM-ALK was even more rapidly degraded upon 17-AAG treatment. Prolonged exposure to the proteasome inhibitor was shown to trigger caspase-3-mediated apoptosis in proliferating ALCL cells at nanomolar concentrations. However, we verified that the accumulation of detergent-insoluble NPM-ALK in ALCL cells was not a spurious consequence of PS341-committed apoptosis, because caspase inhibitors prevented poly(ADP-ribose) polymerase cleavage whereas they did not affect par-titioning of aggregated NPM-ALK. In line with these observations, the carboxyl hsp70-interacting ubiquitin ligase (CHIP), was shown to increase basal ubiquitination and turnover of NPM-ALK kinase, supporting a mechanism whereby NPM-ALK proceeds rapidly toward hsp70-assisted ubiquitin-dependent proteasomal degradation, when chaperoning activity of hsp90 is prohibited by 17-AAG.

INTRODUCTION

Anaplastic large cell lymphomas (ALCLs) show recurring chromosomal translocations between chromosome 2 and chromosomes 1, 3, or 5 and in a few cases, chromosomes 17 and 19 (1). The majority of the anaplastic lymphoma kinase (ALK)-positive ALCLs carries a t(2;5)(p23;q35) reciprocal translocation that originates a M_r 80,000 constitutively active tyrosine kinase protein, termed nucleophosmin (NPM)-ALK or p80, where the oligomerization motif within the NH_2-terminal portion of the NPM protein is juxtaposed to the catalytic domain of the insulin-like ALK tyrosine kinase receptor (2). The oncogenic potential of NPM-ALK has been demonstrated both *in vivo* and *in vitro*, because mice that receive injections of NPM-ALK-transformed murine BaF3 or Fr3T3 cells develop hematological malignancies, and ectopic expression of NPM-ALK accelerates cell cycle entry of rat fibroblasts, which also acquire the capability to grow on semi-solid support (3). Moreover, transgenic mice in which the full-length cDNA of the *npm-alk* gene is under control of the murine CD4 promoter spontaneously develop T-cell lymphomas or plasma cell neoplasms (4) and lethally irradiated interleukin 9 transgenic mice reconstituted with NPM-ALK-transduced mouse bone marrow progenitors develop either B-cell lymphomas or T-cell lymphoblastic lymphomas (5). Cytoplasm-localized NPM-ALK homodimers phosphorylate canonical receptor tyrosine kinase adapter proteins such as Shc, IRS-1, Grb2, or PLCγ1, leading to activation of signaling pathways involved in both cell proliferation and survival (6, 7). Indeed, whereas NPM-ALK association with and phosphorylation of p85 regulatory subunit of phosphatidylinositol 3′-kinase activates Akt and reduces Bad-dependent apoptosis (8, 9), phosphorylation of STAT3 transcription factor results in the up-regulation of antiapoptotic protein Bcl-x_L, as well as in transcription of cell-cycle-related genes (10, 11). We have recently shown that expression of mature NPM-ALK kinase requires the interaction with the molecular chaperone heat shock protein (hsp) 90, and inhibition of the chaperoning activity by the benzoquinone 17-allyl-amino-demethoxygeldanamycin (17-AAG) reduces NPM-ALK content and negatively regulates its signaling pathway in ALCL cells (12). The exact mechanism of NPM-ALK degradation is still unknown, but our previous findings that destabilization of NPM-ALK kinase is preceded by binding hsp70 (a chaperone involved both in folding and proteasomal degradation of certain hsp90-client proteins) led us to speculate in favor of the 26S proteasome as degradation pathway of misfolded NPM-ALK. Several other hsp90 chaperone substrates, such as Akt (13), Raf-1 (14), BCR-ABL (15), and CFTR (16), have been reported to bind hsp70, before degradation, in cells treated with hsp90 inhibitors. The ability of hsp70 to drive protein degradation, rather than folding, depends on the interaction with the E3 ubiquitin ligase carboxyl terminus hsp70-interacting protein (CHIP). CHIP binds to hsp70 through NH_2-terminal tetratricopeptide (TPR) motifs (17) while mediating ubiquitination of chaperone-bound polypeptides through a COOH-terminal U-box domain (18). Here, we demonstrate that the inhibition of proteasome activity prevents 17-AAG-dependent degradation of NPM-ALK, resulting in the accumulation of NPM-ALK kinase in the detergent-insoluble fraction of treated cells. Furthermore, we provide evidence that CHIP ubiquitin ligase associates with NPM-ALK and negatively regulates NPM-ALK steady state in transfected cells by promoting its ubiquitination.

Received 11/11/03; revised 2/10/04; accepted 2/26/04.

Grant support: Consiglio Nazionale delle Ricerche-Ministero Istruzione Università e Ricerca, Settore Oncologia, Legge 449/97, and Fondazione Città della Speranza. P. Bonvini was a recipient of a fellowship from Istituto Oncologico Veneto.

The costs of publication of this article were defrayed in part by the payment of page charges. This article must therefore be hereby marked *advertisement* in accordance with 18 U.S.C. Section 1734 solely to indicate this fact.

Requests for reprints: Paolo Bonvini, Clinica di Oncoematologia Pediatrica, Azienda Ospedaliera-Università di Padova, via Giustiniani 3, 35128 Padova, Italy. Phone: 39-049-8215678; Fax: 39-049-8215679; E-mail: paolobonvini@hotmail.com.

MATERIALS AND METHODS

Cell Culture. The human ALK-positive ALCL cell lines Karpas299 and SR786 and the ALK-negative FE-PD (19) were maintained in RPMI 1640 containing 15% heat-inactivated FCS, 2 mmol/liter glutamine, 100 units/ml penicillin, and 100 μg/ml streptomycin under standard tissue-culture conditions. COS-7 monkey renal epithelial cells were cultivated in Dulbecco's

modified medium, supplemented with 10% heat-inactivated FCS, glutamine, penicillin, and streptomycin, as described above.

Reagents and Antibodies. 17-AAG and pyrazylcarbonyl-Phe-Leu-boronate (PS-341) were obtained from L. Neckers and Edward Mimnaugh (National Cancer Institute, Bethesda, MD). Anti-poly(ADP-ribose) polymerase (PARP) and anti-CHIP antibodies were purchased from Calbiochem-Novabiochem Corp. (San Diego, CA). Monoclonal antiactin IgM ascites and horseradish peroxidase goat antimouse IgM were bought from Oncogene Research Products (Boston, MA). Rabbit polyclonal antihistone deacetylase 1 and monoclonal antiubiquitin (P4D1) antibodies and antiphosphotyrosine (PY99) and anti-hsp70 monoclonal antibodies were from Santa Cruz Biotechnology (Santa Cruz, CA). Anti-ALK (ALKc) and anti-NPM (NPM-376) monoclonal antibodies were a generous gift from Prof. B. Falini (University of Perugia, Perugia, Italy). Caspase inhibitors Z-VAD-FMK, Z-AEVD-FMK, DEVD-CHO, and Z-LEHD-FMK and protease inhibitors *N*-acetyl-L-leucyl-L-leucyl-norleucinal (ALLnL), *N*-acetyl-Leu-Leu-Met-CHO (LLM), pepstatin, [4-(2-aminoethyl) benzenesulfonylfluoride, HCl] (AEBSF), calpeptin, and chathepsin inhibitor I were purchased from Calbiochem. Phenylmethylsulfonyl fluoride was purchased from Sigma-Aldrich Co. (St. Louis, MO). Leupeptin, aprotinin, and rabbit antimouse IgG1 were obtained from CAPPEL (ICN Biomedicals Inc., Costa Mesa, CA). 4′,6-Diamidino-2-phenylindole nucleic acid stain, fluorophore-conjugated goat antimouse (Alexa546), and goat antirabbit (Alexa488) antibodies were bought from Molecular Probes (Eugene, OR). Horseradish peroxidase-conjugated sheep antimouse and donkey antirabbit antibodies were purchased from Amersham Biosciences (Uppsala, Sweden), as well as protein A-Sepharose beads and protein G-Sepharose Fast-Flow beads. BCA protein assay and Western blot chemiluminescence reagents were all from Pierce Chemical Co. (Rockford, IL). Protran nitrocellulose membranes were from Schleicher & Schuell. All of the other chemicals used in this study were purchased from Sigma-Aldrich.

Immunoprecipitation and Immunoblotting. ALCL and COS-7 cells were lysed as described previously (12). In brief, cells were washed twice in ice-cold 1× PBS and incubated on ice for 20 min in 1% Triton X-100 lysis buffer. After high-speed clarification at 4°C, supernatants were recovered, and pellets were resuspended in the same volume of lysis buffer and sonicated on ice. Thirty to 60 μg of lysates from both fractions were loaded onto 10% SDS-PAGE and electrotransferred to nitrocellulose membranes. Alternatively, when immunoprecipitation was performed, 500 μg of lysates were incubated for 2–12 h at 4°C with anti-ALK, anti-CHIP, or anti-hsp70 antibody, where indicated. Immunocomplexes were adsorbed to 30 μl of protein G-Sepharose beads or to 150 μl of protein A-Sepharose beads previously conjugated to rabbit antimouse IgG1 antibody and incubated 2 h at 4°C. The immunoadsorbed pellets were washed in 1% Triton X-100 lysis buffer and heated at 95°C in 1× reducing Laemmli loading buffer, before loading onto SDS-PAGE. To assess NPM-ALK ubiquitination, cell lysates were prepared in radioimmunoprecipitation assay buffer (Triton lysis buffer supplemented with 0.1% SDS, 0.5% sodium deoxycholate, 1 mM phenylmethylsulfonyl fluoride (PMSF), 1 mM sodium orthovanadate, and 10 mM sodium fluoride), and SDS-PAGE resolved samples were transferred onto polyvinylidene difluoride membranes. Proteins were visualized by chemiluminescence using a commercial kit (Pierce Chemical Co.). Films (Hyperfilm; Amersham Biosciences) were scanned, and results were analyzed by using image analysis software (NIH Image).

Preparation of Cytoplasmic and Nuclear Fractions. To obtain purified cytoplasmic and nuclear fractions, cells were processed according to the protocol described by Rosette and Karin (20). After washing in PBS, cells were frozen in dry ice and immediately thawed on ice in pH 7.9 hypotonic buffer [10 mM 4-(2-hydroxyethyl)-1-piperazineethanesulfonic acid, 10 mM KCl, 0.2 mM EDTA, 0.1 mM EGTA, 1 mM DTT, 1 mM phenylmethylsulfonyl fluoride, 20 μg/ml leupeptin, and 20 μg/ml aprotinin]. NP40 (2%) was then added, and cells were further lysed by passing through a 26-gauge needle. Soluble cytoplasmic proteins were recovered by clarification at 10,000 × *g*, whereas intact nuclei were resuspended in pH 7.9 hypertonic buffer [20 mM 4-(2-hydroxyethyl)-1-piperazineethanesulfonic acid, 0.4 M NaCl, 1 mM EDTA, and 1 mM DTT] containing protease inhibitors. Nuclear extracts were recovered from pestle-broken nuclei (Kimble/Kontes Scientific Glassware Instruments, Vineland, NJ), rocked on ice for 30 min, and clarified by high-speed centrifugation (10,000 × *g*). Supernatant represents soluble nuclear extracts.

Preparation of Expression Constructs and Transient Transfection. The whole *npm-alk* coding region, originally cloned into the pSRαMSVtkneo retroviral vector (3), was subcloned into the pcDNA3 vector (Invitrogen). Point mutant NPM-ALK^{K210A} (K210A) was created with QuikChange Site-Directed Mutagenesis Kit system (Stratagene, La Jolla, CA). Wild-type CHIP and the two point mutants K30A and H260Q, cloned into the pcDNA3.1 vector, are kind gifts from L. Neckers. To transiently express the constructs described above, COS-7 cells (0.2×10^6) were plated in 100-mm dishes; after 72 h, log-phase growing cells were transfected with 35 μg each of NPM-ALK or NPM-ALK^{K210} or with 20 μg when either construct was cotransfected with equal amounts of β-galactosidase (β-gal) or CHIP expression vectors, by calcium-phosphate DNA coprecipitation. Thirty-six h after transfection, COS-7 cells were lysed in ice-cold lysis buffer or additionally treated with 17-AAG and/or PS-341, where indicated. Lysates were clarified, immunoprecipitated, and resolved by SDS-PAGE as described above.

Fluorescence Microscopy. Karpas299 cells (3×10^3) were plated onto 8 well/chamber slides (Becton Dickinson, Franklin Lakes, NJ) and grown for 72 h. Cells were then incubated for 24 h with 17-AAG, PS-341, or both compounds, as reported in Fig. 3. Exponentially growing cells were fixed in 3.7% formaldehyde, permeabilized in 0.2% Triton X-100, and blocked in 10% FCS-PBS, followed by incubation in 100 mM glycin. After permeabilization, cells were incubated 1 h at 37°C with ALK-11 rabbit anti-ALK antibody (a kind gift of S. W. Morris, St. Jude Children's Research Hospital, Memphis, TN) and with a mouse antiubiquitin antibody. After extensive washing in PBS, cells were incubated with fluorophore-conjugated secondary antibodies goat antirabbit (Alexa488) and goat antimouse (Alexa546) at a 1:500 dilution of 2 mg/ml stock. Cells were then washed in PBS and mounted onto slides with 1:1 PBS/glycerol, with addition of 4′,6-diamidino-2-phenylindole nucleic acid stain at a 1:1000 dilution. Cells were observed at ×63/0.75 numerical aperature in a Leica DMBL microscope. Images were obtained with a Leica DC 300F digital camera and prepared for reproduction with Leica IM1000 imaging software (Leica Microsystems Ltd., Wetzlar, Germany).

RESULTS

NPM-ALK Accumulates in the Detergent-Insoluble Cell Fraction after Proteasome Inhibition. Degradation of receptor tyrosine kinases still remains an intriguing issue, because immature receptor proteins are usually degraded through the 26S proteasome, whereas proteolysis of mature receptors upon ligand-dependent endocytosis and ubiquitination may be both lysosome and proteasome dependent (21–26). Because we have previously shown that the ALK receptor protein moiety is responsible for the accelerated degradation of NPM-ALK kinase when hsp90-folding activity is inhibited by 17-AAG (12), we screened a panel of selective protease inhibitors. We included inhibitors of both proteasomal and lysosomal function to characterize the degradation pathway of NPM-ALK in 17-AAG-treated ALCL cells Karpas299 and SR786 (Fig. 1, *A* and *B,* respectively). Exponentially growing cells were treated for 8 h with inhibitors of lysosomal (leupeptin and pepstatin), calpain (cathepsin inhibitor I and calpeptin), proteasomal (PS-341, ALLnL and LLM), and serine/threonine (AEBSF, PMSF) proteases in the presence of 10 μM 17-AAG. Surprisingly, none of the inhibitors used had an effect on NPM-ALK expression in the clarified lysates of both cell lines. However, in ALCL cells incubated with proteasome inhibitors PS-341, ALLnL, and LLM, degradation of NPM-ALK caused by 17-AAG was somehow prevented, because NPM-ALK accumulated consistently in detergent-insoluble pellet fractions (Fig. 1, *A* and *B, graph*). Given that boronic acid dipeptides (PS-341) and peptide aldehydes (ALLnL and LLM) are promiscuous inhibitors, because they also target certain serine and cysteine proteases besides the proteasome (27), we analyzed more specific inhibitors of such enzymes AEBSF, cathepsin inhibitor I, and calpeptin. Yet, because no similar accumulation of NPM-ALK protein occurred with such more specific compounds, it is likely that NPM-ALK is subjected to proteasomal degradation when its hsp90-assisted maturation is impeded by 17-AAG.

To investigate the kinetics of NPM-ALK degradation, Karpas299 cells were exposed to 0.5 μM 17-AAG for 24 h, and proteasome activity was inhibited for 16 or 24 h (Fig. 1*C, Lanes 1–7*). Unlike the

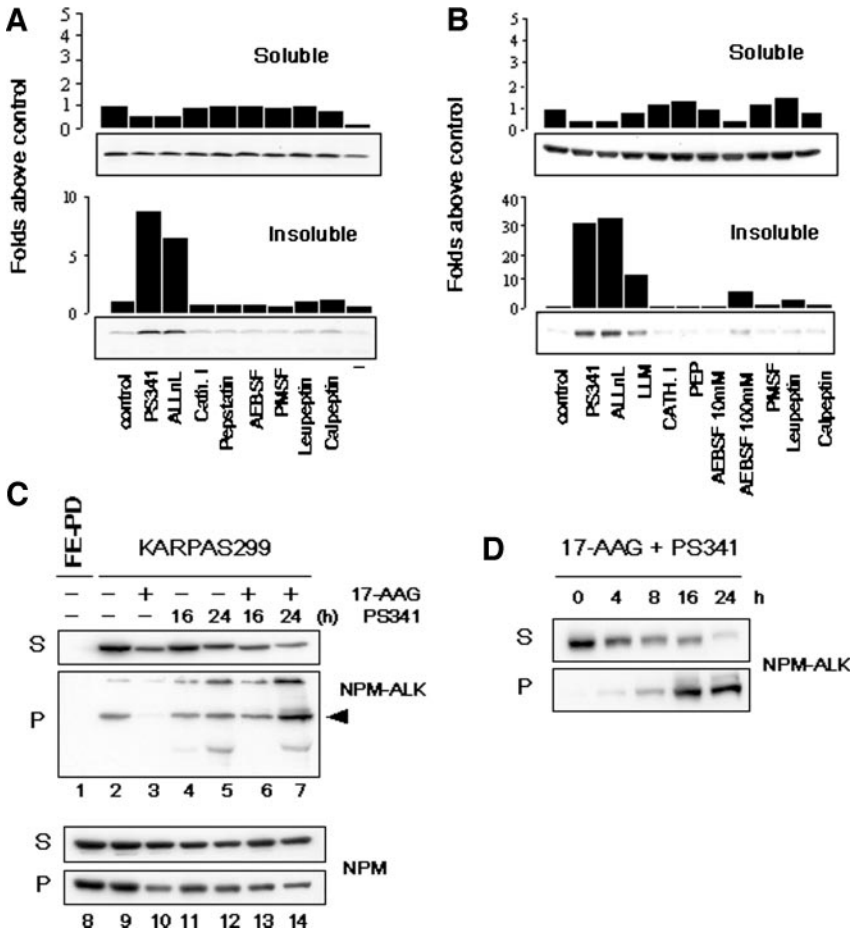

Fig. 1. Effect of protease inhibitors on NPM-ALK steady state in ALCL cell lines. To elucidate the degradation pathway of NPM-ALK, we screened a panel of inhibitors of proteasomal (3 μM PS-341, 100 μM ALLnL, and 100 μM LLM), lysosomal (100 μM leupeptin and 100 μM pepstatin), serine/threonine (10 or 100 μM AEBSF and 2 mM phenylmethylsulfonyl fluoride), and cysteine proteases (20 μM cathepsin inhibitor I and 10 μg/ml calpeptin). Exponentially growing ALCL Karpas299 (*A*) and SR786 (*B*) cells were treated for 8 h with the protease inhibitors, in the presence of 17-AAG (10 μM), or left untreated (*control*). Detergent-soluble and detergent-insoluble fractions were separated as described in "Materials and Methods," and 30 μg of protein lysates were resolved by 10% SDS-PAGE under reducing conditions. Nitrocellulose blots were probed for NPM-ALK and visualized by chemiluminescence technique. Band densities were quantified using image analysis software (NIH image) and expressed as folds above control (*bar graphs*). *C,* time-dependent accumulation of insoluble NPM-ALK was evaluated by exposing Karpas299 cells to 50 nM PS-341 for 16 or 24 h in the presence or absence of 0.5 μM 17-AAG, as indicated in the figure. After purifying both detergent-soluble (*S*) and detergent-insoluble (*P*) fractions, NPM-ALK (*Lanes 2–7*) and NPM (*Lanes 9–14*) expression levels were measured. The t(2;5)-negative ALCL cell line FE-PD was included as a negative control for NPM-ALK (*Lanes 1* and *8*). *D,* Karpas299 cells were treated with 50 nM PS-341 and 0.5 μM 17-AAG for increasing time intervals. NPM-ALK was analyzed by Western blotting of Triton X-100-soluble (*S*) and Triton X-100-insoluble (*P*) fractions.

M_r 38,000 protein NPM (Fig. 1*C, Lanes 8–14*), NPM-ALK protein level was reduced both in clarified lysates and detergent-insoluble pellet fractions after treatment with 17-AAG (Fig. 1*C, Lane 3*). When added to 17-AAG, PS-341 inhibitor did not prevent the down-regulation of detergent-soluble NPM-ALK but caused time-dependent partitioning of NPM-ALK in the insoluble pool (Fig. 1*C, Lanes 6* and *7*). When Karpas299 cells were grown in the presence of both 17-AAG and PS-341 for increasing time intervals, time-dependent down-regulation of soluble NPM-ALK caused by 17-AAG paralleled exactly the up-regulation of insoluble NPM-ALK mediated by PS-341 (Fig. 1*D*), in accordance with what was shown previously for other hsp90-client proteins (28–30).

PS-341-Induced Apoptosis Does Not Affect Proteasomal Degradation of NPM-ALK. PS-341 was the first proteasome inhibitor to enter Phase I clinical trial for its antitumor activity, because tumor cells are more sensitive than normal cells to PS-341-dependent impairment of cell growth and induction apoptosis (31, 32), as recently shown in multiple myeloma cells both *in vivo* and *in vitro* (33, 34). Pro-apoptotic activity of PS-341 was assessed both in t(2;5)-positive (Karpas299, SUDHL1, and SR786) and t(2;5)-negative (FE-PD) ALCL cell lines, by exposing cells for 48 h to nanomolar concentrations of inhibitor. As shown in Fig. 2*A, in vitro* cell proliferation was inhibited by more than 90% at 10 nM in all of the cell lines and regardless of NPM-ALK expression (Fig. 2*A, graph*). Indeed, exposure to PS-341 caused time-dependent cleavage of the M_r 116,000 apoptotic hallmark PARP (Fig. 2*A, panels*) into its caspase-cleaved fragment of M_r 89,000 (Fig. 2*A, arrowheads*) in both ALK-positive (SUDHL1 and SR786) and ALK-negative (FE-PD) cells.

Thus, to rule out that the accumulation of insoluble NPM-ALK might be an artifact of PS-341-driven apoptosis rather than inhibition of its proteasomal degradation, Karpas299 and SR786 cells (Fig. 2*B, Lanes 1–6* and *7–12,* respectively) were treated with two pan-caspase inhibitors before being exposed for as long as 8 h to higher doses of 17-AAG and PS-341. Consistently with PARP cleavage shown in Fig. 2*A,* the two cell lines responded differently to PS-341 treatment, because down-regulation of mature PARP protein was strongly induced in SR786 but not in Karpas299. In SR786 cells pretreated with Z-VAD-FMK and Z-AEVD-FMK inhibitors, caspase-dependent PARP cleavage was completely blocked (Fig. 2*B, graph*), and PARP protein level rose even higher than in untreated cells, which might possess a constitutive caspase activity, as appears from PARP immunoblots of Fig. 2*A*. In contrast, after incubation with both 17-AAG and PS-341, aggregated NPM-ALK was found in the pellet fraction both in the absence of apoptosis (Fig. 2*B, Lanes 4–6*) and when PS-341-induced apoptosis (SR786) was prevented by the two caspase inhibitors (Fig. 2*B, Lanes 10–12*). When Karpas299 cells were treated longer (24 h) with PS-341, extensive PARP cleavage occurred (Fig. 2*C, graph*), and it was totally prevented by the two specific caspase-3 and caspase-9 inhibitors, DEVD-CHO and Z-LEHD-FMK, respectively. However, redistribution of NPM-ALK upon proteasome inhibition observed in the detergent-insoluble fraction of 17-AAG-treated cells (Fig. 2*C, Lane 4*) was not prevented when both caspase-3 and caspase-9 enzymes were inhibited (Fig. 2*C, Lanes 5* and *6*), hence proving that increase of insoluble NPM-ALK and apoptosis are two independent phenomena in PS-341-treated ALCL cells.

NPM-ALK Relocates in Ubiquitin-Rich Perinuclear Structures after Proteasome Inhibition. Covalent attachment of multiple molecules of ubiquitin to specific lysine residues of target proteins is a

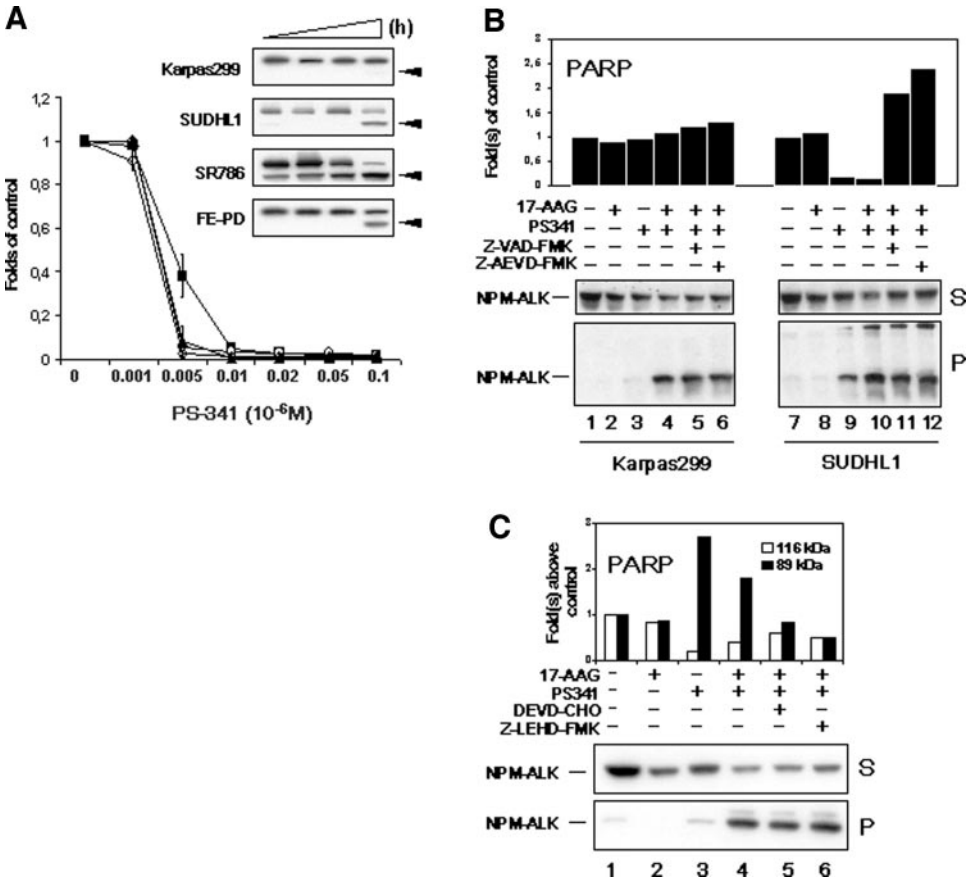

Fig. 2. Effect of PS-341-induced apoptosis on NPM-ALK degradation. *A,* Karpas299 (■), SUDHL1 (○), SR786 (▲), and FE-PD (◆) cell lines were cultured in the presence or absence of PS-341 ($0.001–0.1 \times 10^{-6}$ M) for 48 h. Cell growth was assessed by 3-(4,5-dimethylthiazol-2-yl)-2,5-diphenyltetrazolium bromide assay. Values represent the mean (± SD) of triplicate cultures of three independent experiments. To measure PARP cleavage, ALCL cell lines were treated for 0, 2, 4, and 8 h with 100 nM PS-341. Mature M_r 116,000 PARP protein and its M_r 89,000 cleaved form were visualized by Western blotting. *B,* log-phase growing Karpas299 (*Lanes 1–6*) and SR786 (*Lanes 7–12*) cells were exposed to 17-AAG (10 μM) and/or PS-341 (3 μM) for 8 h, after a 60-min pretreatment with two pan-caspase inhibitors, ZVAD (30 μM) and EAVD (30 μM). NPM-ALK steady state was analyzed from both detergent-soluble (*S*) and detergent-insoluble (*P*) fraction. Immunoblotted PARP protein was quantified by image analysis software and expressed in the bar graphs as folds of control. *C,* similarly, Karpas299 cells were pretreated for 60 min with specific caspase-3 and caspase-9 inhibitors (30 μM DVED-CHO and 30 μM Z-LEHD-FMK, respectively) and then maintained in the presence of 17-AAG (0.5 μM) and/or PS-341 (100 nM) for 24 h. Expression of detergent-soluble (*S*) and detergent-insoluble (*P*) NPM-ALK was analyzed. To evaluate PS-341 apoptotic effect in treated or untreated ALCL cells, band densities of Western blotted mature PARP protein (□) and the M_r 89,000 fragment (■) were expressed as folds of control in the framed graph.

strict prerequisite for recognition and subsequent degradation by the 26S proteasome, and inhibition of the proteasome activity normally leads to accumulation of polyubiquitinated proteins into cells (35). Thus, we performed fluorescent microscopy analysis of ALCL cells stained for NPM-ALK and ubiquitin (Fig. 3*A, panels A–D* and *E–H,* respectively), to verify whether detergent-insoluble NPM-ALK corresponds to deposition of ubiquitinated forms of the protein in cells treated with both 17-AAG and PS-341. As shown in Fig. 3*A,* exposing Karpas299 to PS-341 alone caused accumulation of ubiquitinated proteins into the cytoplasm (Fig. 3*A, panel G*), which had no correspondence with the wide distribution of NPM-ALK (Fig. 3*A, panel C*). On the other hand, when the cells were exposed to both 17-AAG and PS-341, NPM-ALK fluorescence showed a perinuclear distribution that perfectly merged with the ubiquitin staining (Fig. 3*A, panels D, H,* and *N, arrowheads*). Besides, when part of the cells were lysed and cytosolic and nuclear soluble fractions were purified and analyzed together with sonicated detergent-insoluble pellets, accumulation of NPM-ALK was found only in the pellet fraction of cells exposed to both 17-AAG and PS-341 (Fig. 3*B, Lane 12*). This indicates that juxtanuclear-localized NPM-ALK observed in fixed cells represents insoluble ubiquitinated NPM-ALK. Furthermore, we observed that chaperones hsp70 and hsp40, but not hsp90, were increased consistently in the detergent-insoluble fraction of NPM-ALK-transfected cells treated with 17-AAG and PS-341 (data not shown). Because this is consistent with the evidence that, upon prolonged inhibition of proteasome activity, molecular chaperones relocate in large perinuclear structures with polyubiquitinated misfolded client proteins (36, 37), it is likely that the deposition of detergent-insoluble NPM-ALK may result from the impairment of its chaperone-assisted proteasomal degradation.

17-AAG-Induced Degradation of NPM-ALK Is Independent of Its Tyrosine Kinase Activity. Ubiquitin-dependent proteasomal degradation of several hsp90-client proteins has been shown to rely upon interaction with the hsp70 chaperone, independently from their biological functions (38–40). To test whether kinase activity was mandatory for NPM-ALK proteasomal degradation, we generated a kinase-defective mutant of NPM-ALK by replacing lysine 210 of the nucleotide-binding domain with alanine (K210A). Wild-type NPM-ALK and kinase-defective K210A mutant, when transiently expressed in COS-7 cells, displayed comparable steady-state levels, although the K210A mutant failed to react with the antiphosphotyrosine antibody that marked NPM-ALK immunoprecipitates (Fig. 4*A*). As expected, 17-AAG inhibited hsp90-driven maturation of both wild-type NPM-ALK and NPM-ALK K210A, causing their rapid depletion in COS-7 cells (Fig. 4*B, Lane 2*). Nevertheless, when added to 17-AAG, PS-341 prevented the loss of the two misfolded proteins and enhanced the extent of their aggregation in the detergent-insoluble pellet fraction (Fig. 4*B, Lane 8*). Interestingly, the K210A mutant showed enhanced sensitivity to hsp90 inhibition (Fig. 4*B, Lane 2*), similarly to what was found recently for kinase-dead EGFR (41). When the kinetics of the down-regulation of the two proteins were compared, 10 μM 17-AAG led to almost complete depletion of the K210A mutant after just 2 h of treatment, whereas wild-type NPM-ALK was still detectable even after 8 h (Fig. 4*C, arrowhead*).

The Ubiquitin Ligase CHIP Down-Regulates NPM-ALK Kinase Expression. Chaperone-assisted folding requires the cooperation of several scaffold proteins and cofactors of the hsp70 and hsp90 multimolecular chaperone complexes (42). The TPR-containing protein CHIP has been shown to suppress the folding and catalyze the ubiquitination of certain hsp90-client proteins when bound to hsp70,

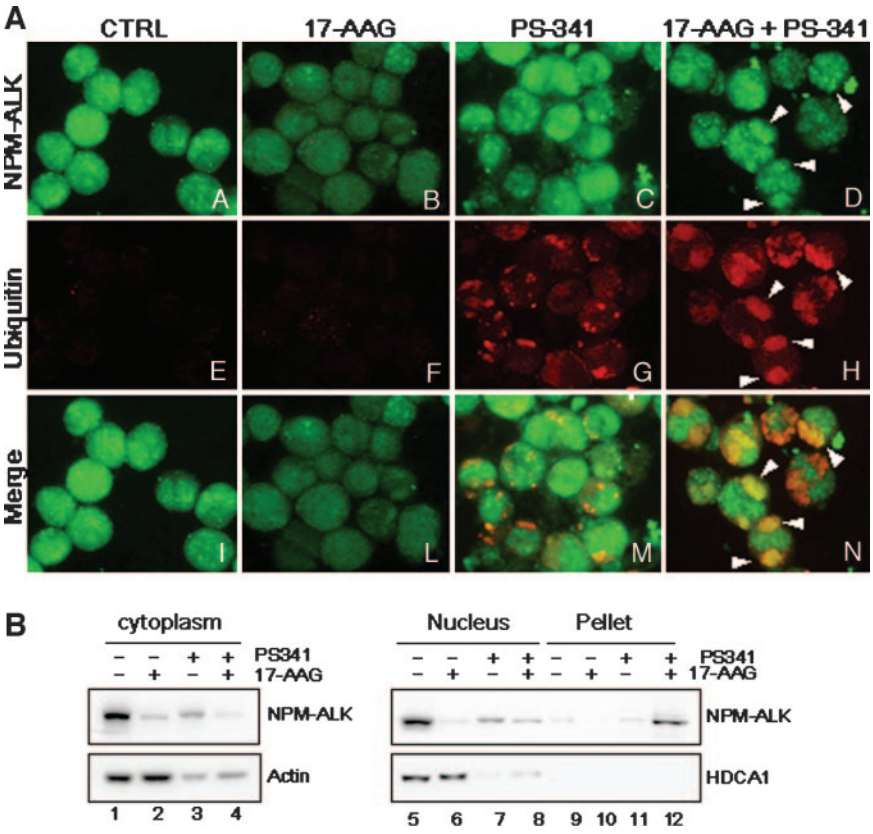

Fig. 3. Cellular localization of NPM-ALK after 17-AAG and PS-341 treatment. *A,* exponentially growing Karpas299 cells were plated onto chamber slides. Cells were treated with 0.5 μM 17-AAG (*panels B, F,* and *L*), 100 nM PS-341 (*panels C, G,* and *M*), or both (*panels D, H,* and *N*). Untreated cells are shown in *panels A, E,* and *I*. After 24 h, cells were processed and analyzed by immunofluorescence technique, using anti-NPM-ALK-specific (*panels A-D*) and anti-ubiquitin-specific (*panels E-H*) monoclonal antibodies. Merge of the two signals is shown in *panels I-N. B,* subfractionation analysis of Karpas299 cells treated with 17-AAG and PS-341 was also performed. Cytosolic (*Lanes 1–4*), nuclear soluble (*Lanes 5–8*), and detergent-insoluble (*Lanes 9–12*) extracts were prepared as described in "Materials and Methods," and NPM-ALK steady state was analyzed by Western blotting. Actin and histone deacetylase 1 proteins were included to assess the integrity of the cytosolic and nuclear-soluble fractions, respectively.

by virtue of a COOH-terminal U-box domain (43, 44). Point mutations at lysine 30 within the TPR domain or at histidine 260 of the U-box domain abrogate respectively CHIP ability to complex with hsp70 and its ubiquitin ligase activity, both mandatory for ubiquitin-dependent proteasomal degradation of chaperone-bound substrates (45). Because we have recently shown that after 17-AAG treatment, NPM-ALK/hsp70 association increases and precedes NPM-ALK down-regulation in ALCL cells, we wondered whether CHIP could regulate NPM-ALK turnover, perhaps throughout hsp70. Therefore, we examined NPM-ALK steady state in COS-7 cells expressing wild-type CHIP or each of the two point mutants described above (CHIP K30A and CHIP H260Q) or β-gal protein. In accordance with our hypothesis, wild-type CHIP protein markedly diminished NPM-ALK expression when compared with β-gal or the two point mutants (Fig. 5*A, Lanes 1–4*), and it stimulated kinase-defective NPM-ALK K210A degradation (Fig. 5*A, Lanes 5–9*). When an anti-CHIP antibody was used for immunoprecipitation, NPM-ALK precipitated from clarified lysates of CHIP-transfected and CHIP H260Q-transfected cells (Fig. 5*B, Lanes 4* and *6*) but not from β-gal or K30A cell lysates (Fig. 5*B, Lanes 2* and *5*). Control immunoprecipitation, performed by immunoadsorbing NPM-ALK with ALK-C antibody, ruled out any spurious effect by detecting NPM-ALK in all of the above described cell lysates, except in lysates of untransfected COS-7 (Fig. 5*B, Lane 8*). In addition, we carried out reverse co-immunoprecipitation and confirmed that, unlike CHIP K30A, wild-type CHIP and CHIP H260Q associated with hsp70 and NPM-ALK (Fig. 5*B, Lanes 13* and *14* and *19* and *20,* respectively) as well as with kinase-defective NPM-ALK K210A (data not shown). Taken together, these data indicate that recruitment of CHIP and subsequent degradation of NPM-ALK kinase depends on NPM-ALK binding to hsp70 rather than on its kinase activity.

Additionally, we investigated the combinatorial effect of CHIP expression and 17-AAG treatment, because we noticed a similar inhibitory effect on NPM-ALK steady state. Indeed, CHIP and 17-AAG seemed to cooperate in this activity, because 17-AAG-induced depletion of soluble NPM-ALK further increased in the presence of CHIP (Fig. 5*C*). In contrast, CHIP H260Q mutant, which lacks enzymatic activity, neither affected soluble NPM-ALK level in untreated cells nor prevented its down-regulation in the presence of 17-AAG. Yet, it is worth pointing out that CHIP may cause apparent down-regulation of hsp90 substrates independently of its ubiquitin ligase activity, by partitioning misfolded hsp90 substrates in the insoluble pool (46). In fact, cotransfection of NPM-ALK with both wild-type CHIP and CHIP H260Q resulted in the redistribution of NPM-ALK from the soluble to the insoluble pool even in the absence of 17-AAG (Fig. 5*C*), whereas exposure to 17-AAG treatment was additive to such an effect.

CHIP Enhances NPM-ALK Ubiquitination in COS-7 Cells. To assess whether CHIP ubiquitin ligase activity stimulates NPM-ALK ubiquitination, COS-7 cells untransfected or transfected with plasmids expressing NPM-ALK, β-gal, or CHIP were incubated with 10 μM 17-AAG, 3 μM PS-341, and the combination thereof for 8 h. As shown in Fig. 6*A,* treating β-gal/NPM-ALK-expressing cells with 17-AAG was enough to elicit NPM-ALK ubiquitination, thus reinforcing the concept that NPM-ALK is efficiently ubiquitinated before proteasome degradation when hsp90-folding activity is inhibited. Blockade of proteasome activity by PS-341 had only a slight effect on NPM-ALK ubiquitination, whereas it enhanced the level stabilized by 17-AAG (Fig. 6*A, Lanes 1–4*). In the presence of CHIP, however, polyubiquitinated NPM-ALK was precipitated even from the clarified lysates of untreated cells, and the extent of NPM-ALK ubiquitination was augmented dramatically after treatment with 17-AAG and PS-341 (Fig. 6*A, Lanes 9–12*). As expected, immunoadsorbed lysates from untransfected (Fig. 6*A, Lanes 5–8*) or β-gal/CHIP-transfected cells (Fig. 6*A, Lanes 13* and *14*) did not contain any higher molecular-weight form of ubiquitinated NPM-ALK, which indicates the relative

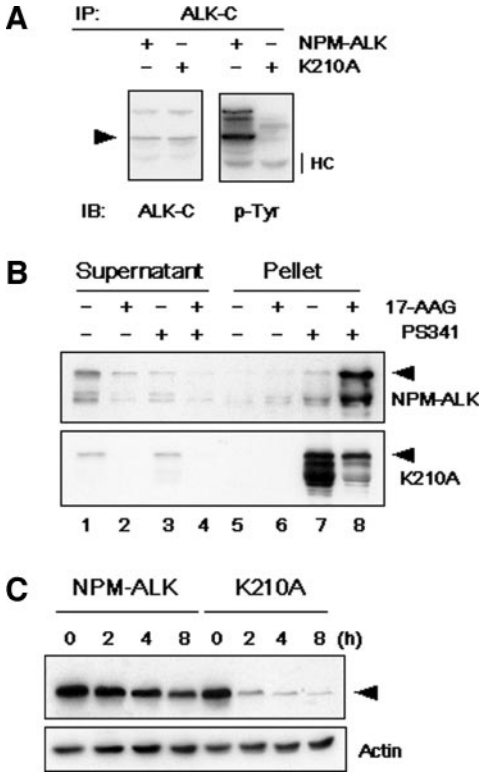

Fig. 4. 17-AAG-mediated proteasomal degradation of NPM-ALK and kinase-dead NPM-ALK K210A in COS7 cells. *A,* wild-type NPM-ALK and NPM-ALK point mutant K210A were transiently transfected (35 μg) into exponentially growing COS7 cells. Protein lysates (500 μg) were precipitated with anti-ALK antibody and then probed for NPM-ALK (ALK-C) or with anti-p-tyrosine antibody (p-Tyr). NPM-ALK proteins are indicated by *arrowheads*; *HC,* heavy chain. *B,* thirty-six h after transfection, COS7 cells were treated for 24 h with 17-AAG (0.5 μM) and/or PS-341 (100 nM). Expression of either NPM-ALK or K210A mutant was determined resolving 60 μg of lysates, from both detergent-soluble and detergent-insoluble fractions, by SDS-PAGE. *C,* time-dependent 17-AAG effect on NPM-ALK and K210A mutant steady state was measured by exposing transfected COS-7 cells to 17-AAG (10 μM) for increasing time periods and resolving 60 μg of total lysates by SDS-PAGE.

specificity of CHIP-induced NPM-ALK ubiquitination. Remarkably, we found that the association between NPM-ALK and CHIP was stabilized by the proteasome inhibitor PS-341 in the presence of 17-AAG (Fig. 6*A, bottom*), although CHIP steady state remained unaltered (Fig. 6*B*). Thus, we can conclude that CHIP supports the ubiquitination of NPM-ALK *per se* and in the presence of 17-AAG, and blockade of the proteasome catalytic activity results in the accumulation of CHIP-bound polyubiquitinated NPM-ALK.

DISCUSSION

NPM-ALK is a M_r 80,000 fusion tyrosine kinase originating from a reciprocal translocation between chromosomes 2 and 5, which regulates cell-cycle progression of ALK-positive ALCL lymphomas (47) and antiapoptotic behavior of transformed cells (3) upon self-association and phosphorylation. Ansamycin drugs such as herbimycin, geldanamycin, and its derivative 17-AAG have been found to diminish NPM-ALK expression and tyrosine phosphorylation in ALCL cells, leading to G_1-phase arrest and apoptosis (48, 49). Despite their initial use as tyrosine kinase inhibitors, ansamycins are a class of small molecules with no inhibitory kinase activity *in vitro* (50) but are capable of binding to and competing with ATP for the ATP-binding site of the molecular chaperone hsp90, which regulates late-stage folding and maturation of several signaling proteins. Drug-induced impairment of hsp90-chaperoning activity has been shown to promote ubiquitin-dependent proteasomal degradation of non-native substrates (51, 52), and we have previously shown that inhibition of hsp90 activity by 17-AAG prevents NPM-ALK/hsp90 complex formation and accelerates NPM-ALK turnover (12).

Covalent attachment of multiple ubiquitin molecules to selected lysine residues targets for ATP-dependent proteolysis by the 26S proteasome both normal native and unfolded proteins, as well as damaged polypeptides (35). However, ubiquitin-dependent degradation of growth factor receptors is still an intriguing process, because

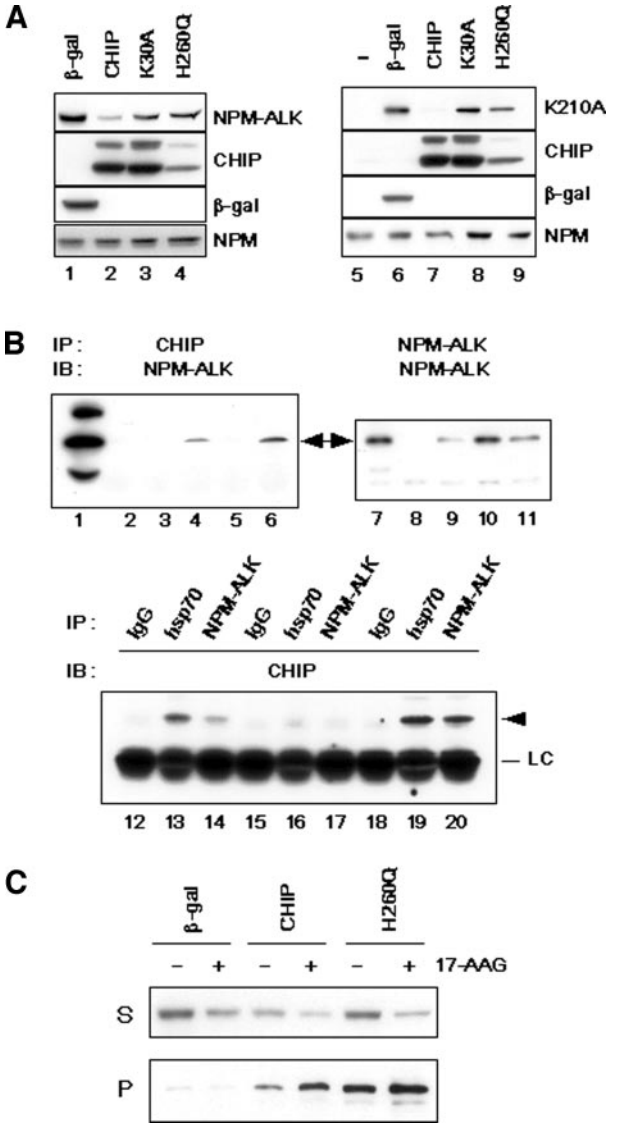

Fig. 5. Effect of CHIP expression on wild-type and kinase-dead NPM-ALK steady state in COS7 cells. *A,* NPM-ALK was transfected into COS7 cells with wild-type CHIP, CHIP K30A, CHIP H260Q, or β-gal. Protein lysates were immunoblotted for NPM-ALK, CHIP, β-gal, and NPM as indicated in figure. *B,* association between CHIP and NPM-ALK was investigated by precipitating 500 μg of protein lysates with 4 μl of CHIP antiserum from β-gal-, CHIP-, K30A- and H260Q-transfected cells (*Lanes 2, 4, 5,* and *6,* respectively). Immunoadsorbed CHIP proteins were resolved by SDS-PAGE, transferred to nitrocellulose filters, and probed for NPM-ALK (*arrow*). Total lysates from NPM-ALK/β-gal-transfected cells and negative controls from untransfected COS-7 cells are shown in *Lanes 1* and *3,* respectively. Control NPM-ALK immunoprecipitation is shown in *Lanes 7–11,* which corresponds to samples 2–6 described above. The association was also demonstrated by reverse immunoprecipitation of 500 μg of COS7 cell lysates with anti-hsp70 or anti-ALK antibody as indicated, from CHIP-, K30A-, and H260Q-transfected cells (*Lanes 12–14, 15–17,* and *18–20,* respectively). Position of exogenous CHIP proteins is indicated by *arrow*; *LC,* light chain; *IgG,* blanks. *C,* combinatorial effect of 17-AAG (10 μM) treatment and CHIP expression on NPM-ALK steady state was analyzed by treating COS-7 cells, cotransfected with β-gal, CHIP, or CHIP H260Q expression vectors, for 8 h. Detergent-soluble (*S*) and detergent-insoluble (*P*) fractions were obtained as described in "Materials and Methods," and NPM-ALK protein level was detected by Western blotting.

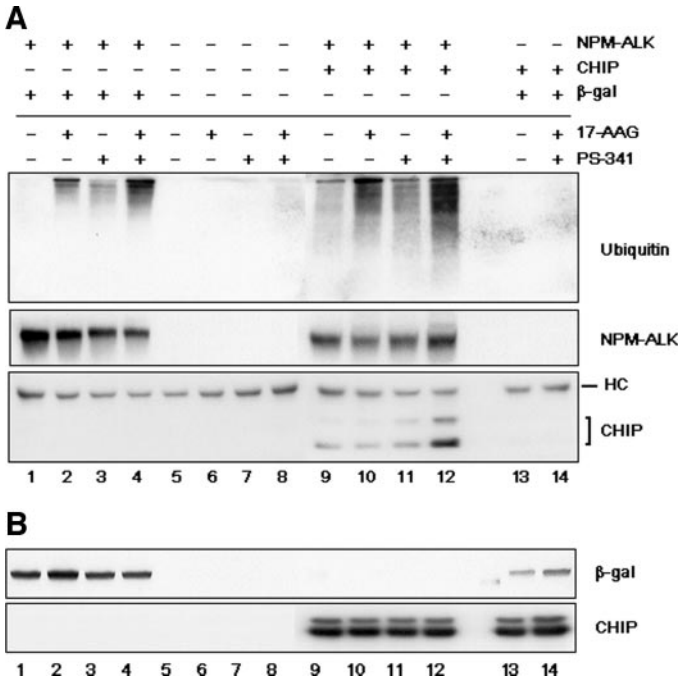

Fig. 6. NPM-ALK ubiquitination in COS-7 cells. *A,* to detect ubiquitinated NPM-ALK, 1 mg of cell lysates of COS7 cells untransfected (*Lanes 5–8*) or cotransfected with NPM-ALK and either β-gal or CHIP expression plasmids (*Lanes 1–4* and *9–12,* respectively) or with β-gal and CHIP (*Lanes 13 and 14*) was precipitated with ALK-C antibody. Samples resolved by SDS-PAGE and transferred onto polyvinylidene difluoride membranes were probed for ubiquitin (*top*), NPM-ALK (*middle*), or CHIP (*bottom*). *HC,* heavy chain. *B,* β-gal and CHIP expression levels in untransfected and transfected COS-7 cells is reported as described in *A*.

poly-ubiquitination of ligand-activated receptors at the plasma membrane has been shown to accelerate endocytosis (22, 53–55), whereas subsequent proteolysis of endosome-sequestered receptors may be hindered either by proteasomal or lysosomal inhibitors (24, 25). To investigate the degradation pathway of NPM-ALK, we screened a panel of lysosomal, endosomal, and proteasomal inhibitors, because the COOH-terminal portion of NPM-ALK corresponds to the entire cytoplasmic domain of the transmembrane receptor ALK, possibly including sequences relevant for both proteasomal and/or lysosomal proteolysis. When the ALCL cell lines Karpas299 and SR786 were maintained in the presence of both 17-AAG and the different protease inhibitors described in Fig. 1, 17-AAG-induced degradation was prevented and NPM-ALK accumulated in the detergent-insoluble fraction only in the presence of proteasome inhibitors. The observation that aggregated NPM-ALK did not accumulate when selective inhibitors of serine, cysteine, and lysosomal proteases were used suggests that the proteasome may represent the preferred degradation pathway of NPM-ALK in 17-AAG-treated cells.

Abrogation of proteasomal activity by PS-341 inhibitor has been found to block cell cycle progression of tumor cells (31, 32) and to induce apoptosis through nuclear factor κB (NFκB) antiapoptotic activity overcome (56), cytochrome *c* release (57), Bcl-2 cleavage (58), and c-Jun NH_2-terminal kinase-dependent caspase-3 and caspase-8 activation (59). The effect, which increases tumor cell sensitivity to DNA-damaging chemotherapy both *in vitro* and *in vivo* (60, 61), can be prevented by pan-caspase or caspase-3 inhibitors (58). In line with these observations, we found that PS-341 did block *in vitro* growth of all of the ALCL cell lines tested, regardless of NPM-ALK kinase expression, and caused apoptosis in a time- and dose-dependent manner, as assessed by caspase-dependent cleavage of PARP protein (Fig. 2*A*). However, even though PS-341-induced fragmentation of PARP was prevented by inactivation of both caspase-3 and caspase-9 (Fig. 2*C*) or by using pan-caspase inhibitors (Fig. 2*B*), aggregated NPM-ALK was still found in the detergent-insoluble pellet fraction of 17-AAG/PS-341-treated cells, proving that proteasomal degradation of NPM-ALK and apoptosis occur independently of each other.

Down-regulation of detergent-soluble NPM-ALK and increase of its detergent-insoluble pool after exposing 17-AAG-treated cells to PS-341 occurred simultaneously in a time-dependent manner (Fig. 1, *C* and *D*), similarly to what was described recently for the hsp90 client protein Akt (28). The loss of solubility seems to be featuring many other misfolded chaperone substrates when their binding to hsp90 is prevented and proteasome activity is sequentially inhibited (15, 29, 30, 62, 63), and this correlates to intracellular deposition of polyubiquitinated protein aggregates with a preferred juxtanuclear distribution (64, 65) into vimentin-surrounded inclusions known as aggresomes (37, 65). Indeed, PS-341 caused accumulation of ubiquitinated proteins in Karpas299 cells, and the extent further increased in the presence of 17-AAG (Fig. 3*A*). PS-341 treatment did not significantly alter steady-state and cellular localization of NPM-ALK fusion kinase in the absence of 17-AAG, but it caused NPM-ALK to colocalize with ubiquitin, when combined to the hsp90 inhibitor, into perinuclear vesicles resembling the polyubiquitinated protein aggregates described (Fig. 3). The data presented above support a mechanism whereby 17-AAG-induced misfolding and degradation of NPM-ALK occurs rapidly and efficiently unless proteasome activity is perturbed, likely indicating a relationship between chaperone-assisted folding of NPM-ALK and the ubiquitin/proteasome pathway.

As recently shown, the balance between protein folding and destruction is reached through the activity of chaperone-bound cofactors, such as CHIP and BAG-1, that diverge misfolded or damaged chaperone-client proteins to proteasomal degradation rather than allowing their folding. CHIP, in particular, acts as an E3 ubiquitin ligase and promotes ubiquitination of hsp90-client proteins by virtue of a COOH-terminal U-box domain (43) that recruits the E2-conjugating enzyme UBCH5a (18). Through multiple TPR repeats, CHIP binds to hsp70 and hsp90 in a mutually exclusive manner, preventing hsp70-folding activity and active hsp90/p23 complex formation, respectively (17). Point mutation analysis has shown that both the TPR repeats and U-box domain are mandatory for CHIP ubiquitin ligase activity, because rapid degradation of misfolded proteins in the presence of wild-type CHIP cannot be elicited by either TPR (CHIP K30A) or U-box (CHIP H260Q) point mutants (44, 45, 64, 66). Consistent with this mechanism, we found that CHIP associated with and increased protein turnover of NPM-ALK when expressed in COS-7 cells (Fig. 5). In contrast, in the presence of CHIP H260Q, which binds stronger to hsp70 and NPM-ALK but shows impaired ubiquitin-ligase activity, or CHIP K30A, which does not bind hsp70, NPM-ALK steady state was unaffected, hence proving that ubiquitin-dependent degradation of NPM-ALK takes place when the mutual interaction between CHIP and hsp70 exists. Interestingly, CHIP and 17-AAG exert a similar effect on NPM-ALK stability, which indicates that although some redundancy is likely to occur, a cooperation between the two mechanisms, as previously found for erbB2 (45, 67), may be feasible. Indeed, when COS-7 cells were exposed to 17-AAG, drug-induced degradation of exogenous NPM-ALK was enhanced in the presence of wild-type CHIP, whereas U-box mutant CHIP H260Q did not counteract 17-AAG-induced depletion of soluble NPM-ALK but rather stabilized its insoluble pool (Fig. 5*C*). By acting as an hsp70-folding inhibitor, CHIP may indeed decrease soluble protein levels without stimulating the ubiquitin-dependent degradation pathway but by causing aggregation of misfolded proteins (46). Accordingly, the partition of aggregated NPM-ALK in the detergent-insoluble pellet fraction was observed in cells expressing wild-type or U-box mutant

CHIP (Fig. 5*C*) but not in those cells transfected with CHIP K30A (data not shown). However, when the ubiquitination status was assessed, we verified that CHIP dramatically raised the content of ubiquitinated NPM-ALK when proteasome activity was inhibited in the presence of 17-AAG (Fig. 6), thus indicating that CHIP represents the E3 ubiquitin ligase responsible for the ubiquitination of misfolded NPM-ALK in 17-AAG-treated cells.

Ubiquitin-dependent down-regulation of activated receptor tyrosine kinases at the plasma membrane has been shown to occur upon recruitment of another E3 ubiquitin ligase, Cbl, although that drives endocytosis and lysosomal degradation of monoubiquitinated receptor proteins (68). Unlike CHIP, Cbl needs to be tyrosine phosphorylated before activation and catalytically inactive tyrosine kinases are not affected by Cbl (24, 69, 70). In contrast, in transiently transfected COS-7 cells, kinase-dead NPM-ALK K210A and CHIP associated (data not shown) and CHIP dictated the down-regulation of kinase-dead NPM-ALK (Fig. 5*A*). Besides, kinase-defective NPM-ALK K210A appeared to be more dependent on hsp90-chaperoning activity than wild-type NPM-ALK, as confirmed by the higher responsiveness to and the enhanced decay rate of K210A mutant in the presence of 17-AAG (Fig. 4). In agreement with our data, kinase-dead EGFR was recently shown to bind to hsp90 with higher affinity than wild-type EGFR and to be more rapidly degraded by the hsp90 inhibitor geldanamycin (41). Similarly, folding and stabilization of newly synthesized kinase-inactive heme-regulated eukaryotic initiation factor kinase has been found to depend on hsp90 and to be sensitive to the inhibitory effect of geldanamycin until its kinase domain is acti vated (71).

In conclusion, the present study strongly supports the hypothesis that 17-AAG-induced down-regulation of NPM-ALK kinase occurs through the ubiquitin/proteasome degradation pathway, because inhibition of proteasome activity by PS-341 prevents the depletion of both endogenous and exogenous NPM-ALK induced by 17-AAG. We have hereby shown that combined inhibition of hsp90 and proteasome activity causes NPM-ALK to accumulate insoluble and to relocate in ubiquitin-rich perinuclear vesicles that, resembling aggresome formations, couple NPM-ALK dislocation to degradation. Furthermore, we found a correlation between chaperone-assisted folding and proteasomal degradation of NPM-ALK by showing that CHIP ubiquitin ligase, when bound to hsp70, associates with and enhances the turnover of ubiquitinated NPM-ALK. Finally, what we find particularly interesting from a pharmacological viewpoint, is that inactivating mutations of kinase activity were found to increase NPM-ALK responsiveness toward inhibitors of the hsp90-chaperoning machinery, which makes the development of NPM-ALK kinase inhibitors a promising anticancer strategy when used in combination with hsp90 inhibitors.

ACKNOWLEDGMENTS

We thank Dr. B. Falini for anti-ALK (ALK-C) and anti-NPM (NPM-376) monoclonal antibodies; Dr. S. W. Morris (St. Jude Children's Research Hospital) for ALK-11 polyclonal antibody; Dr. Martina Boscaro (Education and Communication Office, Istituto Oncologico Veneto) for help in editing the manuscript; and E. Tosato for technical support.

REFERENCES

1. Morris SW, Xue L, Ma Z, Kinney MC. Alk+ CD30+ lymphomas: a distinct molecular genetic subtype of non-Hodgkin's lymphoma. Br J Haematol 2001;113:275–95.
2. Morris SW, Kirstein MN, Valentine MB, et al. Fusion of a kinase gene, ALK, to a nucleolar protein gene, NPM, in non-Hodgkin's lymphoma. Science 1994;263:1281–4.
3. Bischof D, Pulford K, Mason DY, Morris SW. Role of the nucleophosmin (NPM) portion of the non-Hodgkin's lymphoma-associated NPM-anaplastic lymphoma kinase fusion protein in oncogenesis. Mol Cell Biol 1997;17:2312–25.
4. Chiarle R, Gong JZ, Guasparri I, et al. NPM-ALK transgenic mice spontaneously develop T-cell lymphomas and plasma cell tumors. Blood 2003;101:1919–27.
5. Lange K, Uckert W, Blankenstein T, et al. Overexpression of NPM-ALK induces different types of malignant lymphomas in IL-9 transgenic mice. Oncogene 2003;22:517–27.
6. Fujimoto J, Shiota M, Iwahara T, et al. Characterization of the transforming activity of p80, a hyperphosphorylated protein in a Ki-1 lymphoma cell line with chromosomal translocation t(2;5). Proc Natl Acad Sci USA 1996;93:4181–6.
7. Bai RY, Dieter P, Peschel C, Morris SW, Duyster J. Nucleophosmin-anaplastic lymphoma kinase of large-cell anaplastic lymphoma is a constitutively active tyrosine kinase that utilizes phospholipase C-γ to mediate its mitogenicity. Mol Cell Biol 1998;18:6951–61.
8. Bai RY, Ouyang T, Miething C, Morris SW, Peschel C, Duyster J. Nucleophosmin-anaplastic lymphoma kinase associated with anaplastic large-cell lymphoma activates the phosphatidylinositol 3-kinase/Akt antiapoptotic signaling pathway. Blood 2000;96:4319–27.
9. Slupianek A, Nieborowska Skorska M, Hoser G, et al. Role of phosphatidylinositol 3-kinase-Akt pathway in nucleophosmin/anaplastic lymphoma kinase-mediated lymphomagenesis. Cancer Res 2001;61:2194–9.
10. Zhang Q, Raghunath PN, Xue L, et al. Multilevel dysregulation of STAT3 activation in anaplastic lymphoma kinase-positive T/null-cell lymphoma. J Immunol 2002;168:466–74.
11. Zamo A, Chiarle R, Piva R, et al. Anaplastic lymphoma kinase (ALK) activates Stat3 and protects hematopoietic cells from cell death. Oncogene 2002;21:1038–47.
12. Bonvini P, Gastaldi T, Falini B, Rosolen A. Nucleophosmin-anaplastic lymphoma kinase (NPM-ALK), a novel Hsp90-client tyrosine kinase: down-regulation of NPM-ALK expression and tyrosine phosphorylation in ALK(+) CD30(+) lymphoma cells by the Hsp90 antagonist 17-allylamino,17-demethoxygeldanamycin. Cancer Res 2002;62:1559–66.
13. Doong H, Rizzo K, Fang S, Kulpa V, Weissman AM, Kohn EC. CAIR-1/BAG-3 abrogates heat shock protein-70 chaperone complex-mediated protein degradation: accumulation of poly-ubiquitinated hsp90 client proteins. J Biol Chem 2003;278:28490–500.
14. Stancato LF, Silverstein AM, Owens Grillo JK, Chow YH, Jove R, Pratt WB. The hsp90-binding antibiotic geldanamycin decreases Raf levels and epidermal growth factor signaling without disrupting formation of signaling complexes or reducing the specific enzymatic activity of Raf kinase. J Biol Chem 1997;272:4013–20.
15. An WG, Schulte TW, Neckers LM. The heat shock protein 90 antagonist geldanamycin alters chaperone association with p210bcr-abl and v-src proteins before their degradation by the proteasome. Cell Growth Differ 2000;11:355–60.
16. Loo MA, Jensen TJ, Cui L, Hou Y, Chang XB, Riordan JR. Perturbation of Hsp90 interaction with nascent CFTR prevents its maturation and accelerates its degradation by the proteasome. EMBO J 1998;17:6879–87.
17. Ballinger CA, Connell P, Wu Y, et al. Identification of CHIP, a novel tetratricopeptide repeat-containing protein that interacts with heat shock proteins and negatively regulates chaperone functions. Mol Cell Biol 1999;19:4535–45.
18. Jiang J, Ballinger CA, Wu Y, et al. CHIP is a U-box-dependent E3 ubiquitin ligase: identification of Hsc70 as a target for ubiquitylation. J Biol Chem 2001;276:42938–44.
19. del Mistro A, Leszl A, Bertorelle R, et al. A CD30-positive T cell line established from an aggressive anaplastic large cell lymphoma, originally diagnosed as Hodgkin's disease. Leukemia 1994;8:1214–9.
20. Rosette C, Karin M. Cytoskeletal control of gene expression: depolymerization of microtubules activates NF-κB. J Cell Biol 1995;128:1111–9.
21. Sorkin A, Krolenko S, Kudrjavtceva N, et al. Recycling of epidermal growth factor-receptor complexes in A431 cells: identification of dual pathways. J Cell Biol 2001;112:55–63.
22. Mori S, Claesson Welsh L, Okuyama Y, Saito Y. Ligand-induced polyubiquitination of receptor tyrosine kinases. Biochem Biophys Res Commun 1995;213:32–9.
23. Mori S, Kanaki H, Tanaka K, Morisaki N, Saito Y. Ligand-activated platelet-derived growth factor β-receptor is degraded through proteasome-dependent proteolytic pathway. Biochem Biophys Res Commun 1995;217:224–9.
24. Levkowitz G, Waterman H, Zamir E, et al. c-Cbl/Sli-1 regulates endocytic sorting and ubiquitination of the epidermal growth factor receptor. Genes Dev 1998;12:3663–74.
25. Longva KE, Blystad FD, Stang E, Larsen AM, Johannessen LE, Madshus IH. Ubiquitination and proteasomal activity is required for transport of the EGF receptor to inner membranes of multivesicular bodies. J Cell Biol 2002;156:843–54.
26. Authier F, Metioui M, Bell AW, Mort JS. Negative regulation of epidermal growth factor signaling by selective proteolytic mechanisms in the endosome mediated by cathepsin B. J Biol Chem 1999;274:33723–31.
27. Myung J, Kim KB, Crews CM. The ubiquitin-proteasome pathway and proteasome inhibitors. Med Res Rev 2001;21:245–73.
28. Basso AD, Solit DB, Chiosis G, Giri B, Tsichlis P, Rosen N. Akt forms an intracellular complex with heat shock protein 90 (Hsp90) and Cdc37 and is destabilized by inhibitors of Hsp90 function. J Biol Chem 2002;277:39858–66.
29. Whitesell L, Sutphin P, An WG, Schulte T, Blagosklonny MV, Neckers LM. Geldanamycin-stimulated destabilization of mutated p53 is mediated by the proteasome in vivo. Oncogene 1997;14:2809–16.
30. Schulte TW, An WG, Neckers LM. Geldanamycin-induced destabilization of Raf-1 involves the proteasome. Biochem Biophys Res Commun 1997;239:655–9.
31. Drexler HC. Activation of the cell death program by inhibition of proteasome function. Proc Natl Acad Sci USA 1997;94:855–60.
32. An B, Goldfarb RH, Siman R, Dou QP. Novel dipeptidyl proteasome inhibitors overcome Bcl-2 protective function and selectively accumulate the cyclin-dependent kinase inhibitor p27 and induce apoptosis in transformed, but not normal, human fibroblasts. Cell Death Differ 1998;5:1062–75.

33. Adams J, Palombella VJ, Sausville EA, et al. Proteasome inhibitors: a novel class of potent and effective antitumor agents. Cancer Res 1999;59:2615–22.
34. Mitsiades N, Mitsiades CS, Richardson PG, et al. The proteasome inhibitor PS-341 potentiates sensitivity of multiple myeloma cells to conventional chemotherapeutic agents: therapeutic applications. Blood 2003;101:2377–80.
35. Glickman MH, Ciechanover A. The ubiquitin-proteasome proteolytic pathway: destruction for the sake of construction. Physiol Rev 2002;82:373–428.
36. Garcia-Mata R, Bebok Z, Sorscher EJ, Sztul ES. Characterization and dynamics of aggresome formation by a cytosolic GFP-chimera. J Cell Biol 1999;146:1239–54.
37. Wigley WC, Fabunmi RP, Lee MG, et al. Dynamic association of proteasomal machinery with the centrosome. J Cell Biol 1999;145:481–90.
38. Bercovich B, Stancovski I, Mayer A, et al. Ubiquitin-dependent degradation of certain protein substrates in vitro requires the molecular chaperone Hsc70. J Biol Chem 1997;272:9002–10.
39. Hohfeld J, Cyr DM, Patterson C. From the cradle to the grave: molecular chaperones that may choose between folding and degradation. EMBO Rep 2001;2:885–90.
40. Young JC, Moarefi I, Hartl FU. Hsp90: a specialized but essential protein-folding tool. J Cell Biol 2001;154:267–74.
41. Citri A, Alroy I, Lavi S, et al. Drug-induced ubiquitylation and degradation of ErbB receptor tyrosine kinases: implications for cancer therapy. EMBO J 2002;21:2407–17.
42. Richter K, Buchner J. Hsp90: Chaperoning signal transduction. J Cell Physiol 2001;188:281–90.
43. Murata S, Minami Y, Minami M, Chiba T, Tanaka K. CHIP is a chaperone-dependent E3 ligase that ubiquitylates unfolded protein. EMBO Rep 2001;2:1133–8.
44. Demand J, Alberti S, Patterson C, Hohfeld J. Cooperation of a ubiquitin domain protein and an E3 ubiquitin ligase during chaperone/proteasome coupling. Curr Biol 2001;11:1569–77.
45. Xu W, Marcu M, Yuan X, Mimnaugh E, Patterson C, Neckers LM. Chaperone-dependent E3 ubiquitin ligase CHIP mediates a degradative pathway for c-ErbB2/Neu. Proc Natl Acad Sci USA 2002;99:12847–52.
46. Jiang J, Cyr D, Babbitt RW, Sessa WC, Patterson C. Chaperone-dependent regulation of eNOS intracellular trafficking by the co-chaperone/ubiquitin ligase CHIP. J Biol Chem 2003 Dec 5;278:49332–41. Epub 2003 Sep 24.
47. Leoncini L, Lazzi S, Scano D, et al. Expression of the ALK protein by anaplastic large-cell lymphomas correlates with high proliferative activity. Int J Cancer 2000;86:777–81.
48. Ergin M, Denning MF, Izban KF, et al. Inhibition of tyrosine kinase activity induces caspase-dependent apoptosis in anaplastic large cell lymphoma with NPM-ALK (p80) fusion protein. Exp Hematol 2001;29:1082–90.
49. Turturro F, Arnold MD, Frist AY, Pulford K. Model of inhibition of the NPM-ALK kinase activity by herbimycin A. Clin Cancer Res 2002;8:240–5.
50. Whitesell L, Mimnaugh EG, De Costa B, Myers CE, Neckers LM. Inhibition of heat shock protein HSP90-pp60v-src heteroprotein complex formation by benzoquinone ansamycins: essential role for stress proteins in oncogenic transformation. Proc Natl Acad Sci USA 1994;91:8324–8.
51. Mimnaugh EG, Chavany C, Neckers L. Polyubiquitination and proteasomal degradation of the p185$^{c\text{-}erbB\text{-}2}$ receptor protein-tyrosine kinase induced by geldanamycin. J Biol Chem 1996;271:22796–801.
52. Imamura T, Haruta T, Takata Y, et al. Involvement of heat shock protein 90 in the degradation of mutant insulin receptors by the proteasome. J Biol Chem 1998;273:11183–8.
53. Mori S, Heldin CH, Claesson-Welsh L. Ligand-induced ubiquitination of the platelet-derived growth factor β-receptor plays a negative regulatory role in its mitogenic signaling. J Biol Chem 1993;268:577–83.
54. Miyake S, Mullane-Robinson KP, Lill NL, Douillard P, Band H. Cbl-mediated negative regulation of platelet-derived growth factor receptor-dependent cell proliferation: a critical role for Cbl tyrosine kinase-binding domain. J Biol Chem 1999;274:16619–28.
55. Stang E, Johannessen LE, Knardal SL, Madshus IH. Polyubiquitination of the epidermal growth factor receptor occurs at the plasma membrane upon ligand-induced activation. J Biol Chem 2000;275:13940–7.
56. Cusack JCJ, Liu R, Houston M, et al. Enhanced chemosensitivity to CPT-11 with proteasome inhibitor PS-341: implications for systemic nuclear factor-κB inhibition. Cancer Res 2001;61:3535–40.
57. Ling YH, Liebes L, Jiang JD, et al. Mechanisms of proteasome inhibitor PS-341-induced G_2-M-phase arrest and apoptosis in human non-small cell lung cancer cell lines. Clin Cancer Res 2003;9:1145–54.
58. Ling YH, Liebes L, Ng B, et al. PS-341, a novel proteasome inhibitor, induces Bcl-2 phosphorylation and cleavage in association with G_2-M phase arrest and apoptosis. Mol Cancer Ther 2002;1:841–9.
59. Hideshima T, Mitsiades C, Akiyama M, et al. Molecular mechanisms mediating antimyeloma activity of proteasome inhibitor PS-341. Blood 2003;101:1530–4.
60. LeBlanc R, Catley LP, Hideshima T, et al. Proteasome inhibitor PS-341 inhibits human myeloma cell growth in vivo and prolongs survival in a murine model. Cancer Res 2002;62:4996–5000.
61. Mitsiades N, Mitsiades CS, Poulaki V, et al. Molecular sequelae of proteasome inhibition in human multiple myeloma cells. Proc Natl Acad Sci USA 2002;99:14374–9.
62. Yorgin PD, Hartson SD, Fellah AM, et al. Effects of geldanamycin, a heat-shock protein 90-binding agent, on T cell function and T cell nonreceptor protein tyrosine kinases. J Immunol 2000;164:2915–23.
63. Vanaja DK, Mitchell SH, Toft DO, Young CY. Effect of geldanamycin on androgen receptor function and stability. Cell Stress Chaperones 2002;7:55–64.
64. Meacham GC, Patterson C, Zhang W, Younger JM, Cyr DM. The Hsc70 co-chaperone CHIP targets immature CFTR for proteasomal degradation. Nat Cell Biol 2001;3:100–5.
65. Johnston JA, Ward CL, Kopito RR. Aggresomes: a cellular response to misfolded proteins. J Cell Biol 1998;143:1883–98.
66. Connell P, Ballinger CA, Jiang J, et al. The co-chaperone CHIP regulates protein triage decision mediated by heat-shock proteins. Nat Cell Biol 2001;3:93–6.
67. Zhou P, Fernandes N, Dodge IL, et al. ErbB2 degradation mediated by the co-chaperone protein CHIP. J Biol Chem 2003;278:13829–37.
68. Haglund K, Sigismund S, Polo S, Szymkiewicz I, Di Fiore PP, Dikic I. Multiple monoubiquitination of RTKs is sufficient for their endocytosis and degradation. Nat Cell Biol 2003;5:461–6.
69. Yokouchi M, Kondo T, Sanjay A, et al. Src-catalyzed phosphorylation of c-Cbl leads to the interdependent ubiquitination of both proteins. J Biol Chem 2001;276:35185–93.
70. Rao N, Miyake S, Reddi AL, et al. Negative regulation of Lck by Cbl ubiquitin ligase. Proc Natl Acad Sci USA 2002;99:3794–9.
71. Uma S, Hartson SD, Chen JJ, Matts RL. Hsp90 is obligatory for the heme-regulated eIF-2α kinase to acquire and maintain an activable conformation. J Biol Chem 1997;272:11648–56.